Mechanistic insights into plant community responses to environmental variables: genome size, cellular nutrient investments, and metabolic tradeoffs

Erika I. Hersch-Green[1], Philip A. Fay[2], Hailee B. Hass[1,3] and Nicholas G. Smith[4]

[1]Department of Biological Sciences, Michigan Technological University, Houghton, MI 49931, USA; [2]USDA ARS Grassland Soil and Water Research Lab, Temple, TX 76502, USA; [3]Department of Biological Sciences, University of Alabama, Tuscaloosa, AL 35487, USA; [4]Department of Biological Sciences, Texas Tech University, Lubbock, TX 79409, USA

Author for correspondence:
Erika I. Hersch-Green
Email: eherschg@mtu.edu

Received: *7 September 2024*
Accepted: *9 December 2024*

New Phytologist (2024)
doi: 10.1111/nph.20374

Key words: climate, genome size, material costs, nutrient enrichment, photosynthesis, stomata, transpiration, water-use efficiency.

Summary

- Affecting biodiversity, plants with larger genome sizes (GS) may be restricted in nutrient-poor conditions. This pattern has been attributed to their greater cellular nitrogen (N) and phosphorus (P) investments and hypothesized nutrient–investment tradeoffs between cell synthesis and physiological attributes associated with growth. However, the influence of GS on cell size and functioning may also contribute to GS-dependent growth responses to nutrients.
- To test whether and how GS is associated with cellular nutrient, stomata, and/or physiological attributes, we examined > 500 forbs and grasses from seven grassland sites conducting a long-term N and P fertilization experiment.
- Larger GS plants had increased cellular nutrient contents and larger, but fewer stomata than smaller GS plants. Larger GS grasses (but not forbs) also had lower photosynthetic rates and water-use efficiencies. However, nutrients had no direct effect on GS-dependent physiological attributes and GS-dependent physiological changes likely arise from how GS influences cells. At the driest sites, large GS grasses displayed high water-use efficiency mostly because transpiration was reduced relative to photosynthesis in these conditions.
- We suggest that climatic conditions and GS-associated cell traits that modify physiological responses, rather than resource–investment tradeoffs, largely explain GS-dependent growth responses to nutrients (especially for grasses).

Introduction

Angiosperms (flowering plants) show tremendous variance in genome sizes (GS) both within and among species (Dodsworth *et al*., 2015; Pellicer *et al*., 2018) and GS variation can alter community eco-evolutionary dynamics. Recent studies have found that angiosperm GS can influence productivity and biodiversity responses to nutrient availabilities such that nutrient-limiting conditions favor the fitness and growth of smaller GS plants, whereas nutrient enrichments have opposite effects and favor the fitness and growth of larger GS plants (Smarda *et al*., 2013; Guignard *et al*., 2016; Bales & Hersch-Green, 2019; Walczyk & Hersch-Green, 2019, 2023; Anneberg & Segraves, 2020; Peng *et al*., 2022). These patterns have, in part, been attributed to hypothesized GS-dependent differences in cellular nitrogen (N) and phosphorus (P) requirements (aka 'material costs') that are predicted to more strongly constrain the growth of larger GS plants under nutrient limitations (Lewis, 1985; Leitch & Bennett, 2004; Cavalier-Smith, 2005; Mei *et al*., 2018; Simonin & Roddy, 2018). By contrast, under nutrient enrichments, larger GS plants are thought to benefit more from growth via cell expansion and/or heterosis, as in the case of allopolyploids (Faizullah *et al*., 2021). Increased cellular nutrient requirements of larger genome organisms are thought to arise because GS scales positively with DNA content and cell sizes (Beaulieu *et al*., 2008; Mueller, 2015; Simonin & Roddy, 2018; Roddy *et al*., 2020), and more N and P atoms are needed for the synthesis of longer strands of nucleic acids, sugar-phosphate backbones (Sterner & Elser, 2002; Elser *et al*., 2011), and phospholipid bilayer cell membranes. However, across phylogenetically divergent lineages and independently of polyploidy, there is very limited information as to whether foliar nutrient investments scale with GS (Jeyasingh & Weider, 2007; Kang *et al*., 2015) or the mechanistic bases for observed GS-dependent growth responses to nutrients.

Photosynthesis and transpiration are integral to plant growth and examining whether GS affects these processes could provide mechanistic insights into determining when GS-dependent growth responses to nutrients are most probable. These processes are likely to be influenced by GS independently of nutrient availability because stomatal attributes vary across diverse plant lineages dependent upon GS, with smaller but more numerous stomata being associated with smaller GS plants (Knight &

Beaulieu, 2008; Liu *et al*., 2017; Simonin & Roddy, 2018; Roddy *et al*., 2020; Théroux-Rancourt *et al*., 2021). Furthermore, smaller and more numerous stomata and overall increases in stomatal pore volumes are associated with higher rates of stomatal conductance, photosynthesis, and transpiration (Franks & Beerling, 2009; Drake *et al*., 2013; Lawson & Blatt, 2014; Harrison *et al*., 2020). GS may also influence gas diffusion rates within plant tissues because larger GS plants tend to have larger cells (Beaulieu *et al*., 2008; Roddy *et al*., 2020) with lower packing densities and reduced surface area to volume ratios that have been associated with slower gas diffusion rates across cell boundaries (Roddy *et al*., 2020; Théroux-Rancourt *et al*., 2021). Therefore, due to GS-dependent 'physiological constraints' (e.g. lower gas uptake from the atmosphere and diffusion capacities), larger GS plants might have lower rates of photosynthesis and transpiration than smaller GS plants, and lower photosynthesis and transpiration rates of larger GS plants have been reported (Beaulieu *et al*., 2008; Herben *et al*., 2012; Roddy *et al*., 2020; Théroux-Rancourt *et al*., 2021; Walczyk & Hersch-Green, 2023).

Site soil nutrient availabilities and specific plant characteristics affecting nutrient requirements might further influence whether and to what extent GS affects photosynthesis, transpiration, and/or the balance between these processes. For instance, the proteins, pigments, ATP, and electron transport molecules used in photosynthesis require significant N and P atoms (Evans, 1989; Hessen *et al*., 2010; Hohmann-Marriott & Blankenship, 2011) and many species have higher rates of photosynthesis and productivity under nutrient enrichments (Vaitkus *et al*., 1993; Liang *et al*., 2020; Shen *et al*., 2022). Thus, especially in nutrient-limiting conditions, N and P investments into macromolecules involved in photosynthesis might compete with investments into nucleic acids and cell synthesis (aka 'material costs'), with these resource allocation tradeoffs being most intense for larger GS plants (Faizullah *et al*., 2021). However, because most transpiration occurs through stomatal pores (Jarvis & Mcnaughton, 1986; Marschner, 2011; Xu *et al*., 2019) and stomatal conductance and gas diffusion between cells should be less dependent on nutrient inputs than photosynthesis, we might expect that GS-associated resource allocation tradeoffs would have minimal effects on transpiration. GS–resource allocation tradeoffs affecting photosynthesis rates may also be influenced by a plant's photosynthetic pathway. For instance, while anatomical and chemical adaptations of C_4 plants are energetically and metabolically more intensive than C_3 plants, C_4 plants tend to be more efficient at conserving and using water and nutrients for photosynthesis than C_3 plants (Brown & Rickless, 1949; Monson, 1989; Taylor *et al*., 2010; Zhao *et al*., 2022). Lastly, to maximize growth and fitness, plants must balance the amount of carbon (C) accumulated for photosynthesis relative to water lost from transpiration (measured as water-use efficiency, WUE), and thus, ultimately, GS-dependent responses to nutrients may depend upon tradeoffs that vary depending upon a plant's GS, photosynthetic pathway, site nutrient availability, and/or prevailing climatic conditions.

To enhance mechanistic understandings of observed GS-dependent growth responses to nutrients, we examined whether GS *per se* influences cellular nutrient contents and whether GS is correlated with metabolic processes associated with growth and survival. We collected GS, cellular nutrient content, stomata size, stomata density, and gas exchange data from > 500 forbs and grasses that occurred at seven grassland sites spanning a north–south environmental gradient in Midwestern United States. Each site was fertilized once per year with identical amounts of N and P in a factorial design (NutNet; https://nutnet.org). We tested five interrelated hypotheses: Cellular C, N, and P contents (aka 'material costs') increase with plant GS, arising from them having larger cells that contain more DNA (H1); larger GS plants have larger and fewer stomata ('physiological constraints', H2); because of increased physiological constraints, larger GS plants have lower rates of photosynthesis especially under nutrient-limiting conditions when resource–investment tradeoffs between cell/nucleic acid syntheses and photosynthesis are the most intense (H3); because of physiological constraints, larger GS plants have lower transpiration rates (H4); and WUE decreases with GS when resource–investment tradeoffs and physiological constraints on cells more strongly affect photosynthesis than transpiration (H5a), does not change with GS when photosynthesis and transpiration are equally affected by the combined resource–investment and physiological constraints on cells or when GS is not correlated with either (H5b), and increases with GS when physiological constraints on cells have greater impacts on transpiration than resource–investment tradeoffs and physiological constraints combined have on photosynthesis (H5c, Fig. 1).

Materials and Methods

Experimental design and site measurements

This study was conducted across seven grassland sites situated along a North–South transect in Midwestern United States. All sites are part of the Nutrient Network (https://nutnet.org), a globally distributed experiment in which plots are fertilized annually using a standard protocol (Borer *et al*., 2014) that allows rigorous cross-site comparisons of the effects of nutrients on biodiversity. The sites chosen varied in latitude, longitude, mean annual precipitation (MAP) and mean annual temperature (MAT); MAP and MAT were extracted at the 30 arc second scale from WORLDCLIM v.2, (Fick & Hijmans, 2017) (Supporting Information Table S1). At each site, we collected measurements from plants that occurred in one of four treatment plots that were replicated across three blocks (total = 12 plots/site): unfertilized control (Cont.), nitrogen-added (N), phosphorus-added (P), and nitrogen- and phosphorus-added (NP). Treatments were randomly assigned to 25-m^2 plots in fully factorial combinations with site coordinators having applied N and P fertilization treatments before the growing season annually at a rate of 10 g m^{-2} (for experimental design details see Borer *et al*., 2014); the length of time since the nutrient treatments were first initiated ranged from 2–15 yr before we collected data (Table S1).

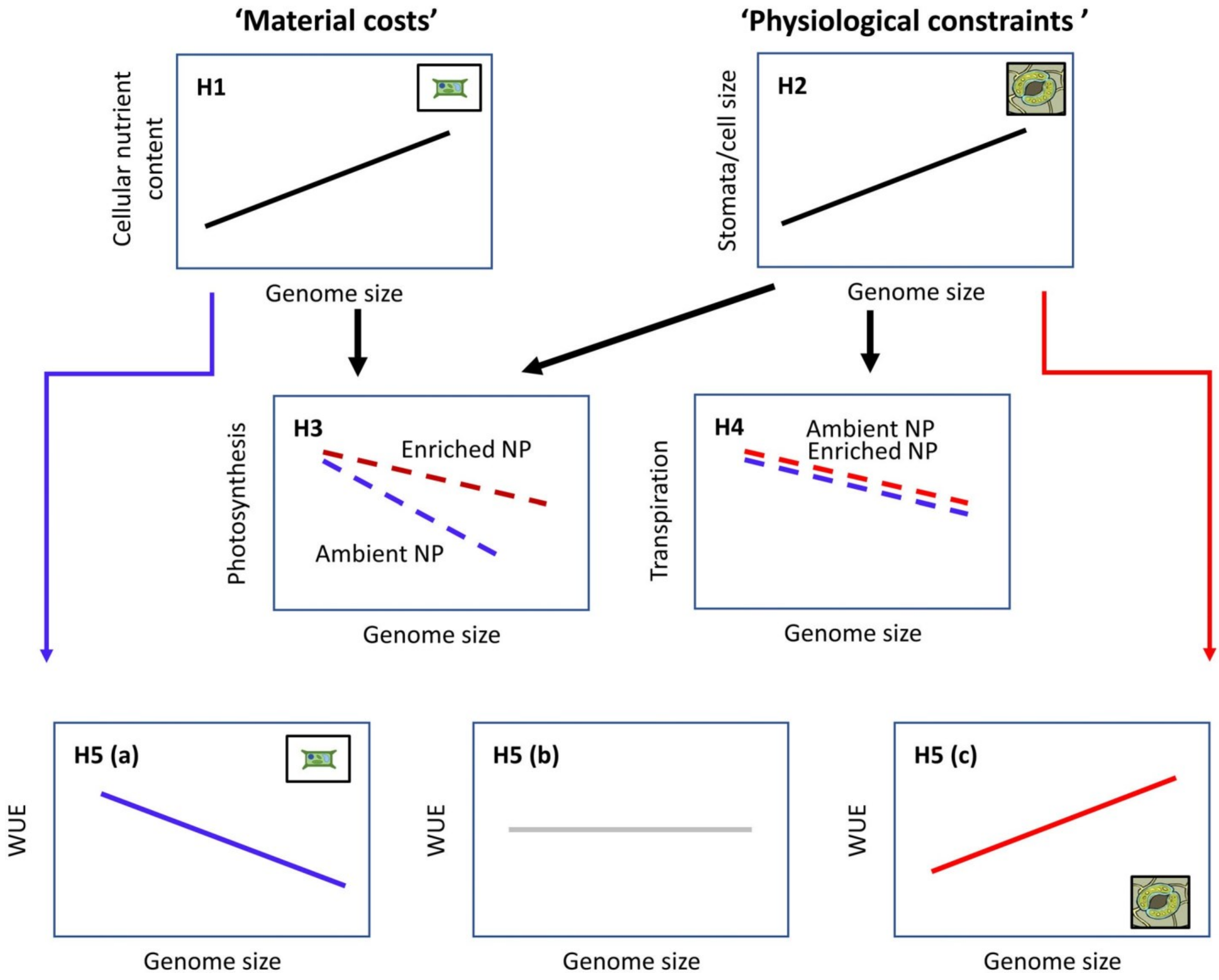

Fig. 1 Hypothesis (H) of relationships between genome size (GS) and gas exchange properties. (H1) Material costs defined – the amount of nitrogen (N) and phosphorus (P) per cell are expected to increase with GS. (H2) Physiological constraints defined – stomata and cell sizes are expected to increase with GS. (H3) Photosynthesis rates are expected to decline with GS as a result of material costs and physiological constraints, but declines are expected to be moderated under NP enrichments due to the weakening of resource–investment tradeoffs. (H4) Transpiration rates are expected to decline with GS as a result of physiological constraints. Water-use efficiency (WUE) is (H5a) expected to decline with GS if resource–investment tradeoffs and material cost constraints are stronger than physiological constraints in affecting metabolic rates, (H5b) expected to not change with GS if gas exchange properties are equally affected by resource–investment and physiological constraints or when GS is not correlated with either, and (H5c) expected to increase with GS if physiological constraints have a greater impact on transpiration than resource–investment tradeoffs and physiological constraints combined have on photosynthesis.

Individual plant and species measurements

At each site, we collected leaves to estimate foliar nutrient contents and measured leaf gas exchange on 6–10 of the most common plants in each plot, with the intention of measuring the same taxa across multiple treatment plots per site. Adjacent to, but outside of, the treatment plots, we also collected four to six fresh leaves from species in which we obtained individual plant measurements to obtain 'site-specific species-level' GS, cell density, and stomata data. All data were collected around site-specific peak biomass, which ranged from May through August 2022 (Table S1).

Genome size From site-specific species-level leaf collections, we measured holoploid GS (2C DNA content, total amount of DNA in un-replicated chromosome sets, Greilhuber *et al*., 2005) by co-chopping samples with internal standards (Doležel *et al*., 2007) and then using flow cytometry (Accuri Inc Ann Arbor, MI, USA) to determine 2C-DNA content values. The details of buffers and internal standards are given in Methods S1. Low-quality samples (CV of flow histogram peaks > 5%) were removed before statistical analysis and species-level, site-specific GS values from 112 taxa (85 forbs and 27 grasses) are given in Table S2.

Cellular foliar nutrients We collected approximately two leaves (exact number depended on leaf architecture) from the upper portion (mostly forbs) or the middle rosette (mostly grasses) of each plant that was measured for photosynthesis and transpiration and combined leaves for each species per site collected from the same treatment plots (Cont, N, P, or NP). We then ground and homogenized the combined leaves and determined foliar [C] and [N] with an elemental analyzer (Costech Analytical Technologies, Valencia, CA, USA) and foliar [P] with acid digestion (Masson *et al*., 2010) on a Thermo 6500 Duo Inductively Coupled Plasma Spectrometer (Thermo-Fischer Scientific, Waltham, MA, USA); total sample sizes for foliar [P] were lower because the process requires more tissue (for [C] and [N]: $n = 460$, for [P]: $n = 268$). From site-specific species-level leaf collections, we took two adjacent leaf punches from plants: one was dried, and one was weighed and digested in 10% chromic acid where we counted and averaged the number of cells in three 10 μl aliquots of a 100 μl solution using a hemocytometer (Brown & Rickless, 1949; Walczyk & Hersch-Green, 2023). We then divided the number of cells by dry mass of the undigested leaf punch to get cell density per milligram of dry tissue. Dividing foliar C, N, or P content measurements in nanogram per milligram of dry tissue by cell density provided site-treatment-species-specific cellular foliar [C], [N] and [P] in ng per cell.

Stomata characteristics From site-specific species-level leaf collections, we calculated average stomata size (μm^2, guard cell length multiplied by width of four randomly selected stomata at ×1000 total magnification) and density (number of stomata present in the field of view at ×400 total magnification) using an Olympus light microscope (Olympus Corp., Shinjuku, Tokyo, Japan); see methods in Hull-Sanders *et al*. (2009) and Walczyk & Hersch-Green (2022).

Photosynthesis, transpiration, and water-use efficiency attributes We used a portable infrared CO_2 analyzer system (LI-6800; Li-Cor Inc., Lincoln, NE, USA) equipped with a CO_2 mixer and 1 × 3 cm^2 chamber/red-blue LED light source to measure net photosynthetic C assimilation rates (A_{sat}, μmol CO_2 m^{-2} s^{-1}) and instantaneous transpiration rates (E, mmol H_2O m^{-2} s^{-1}). All measurements were taken from the youngest set of fully matured leaves over 3–5 days between the hours of 08:00 and 16:00 with care to avoid damaged leaves and cloudy, windy, or hot conditions. Inside the chamber, we set the CO_2 concentration to 420 ppm, relative humidity to 50%, flow rate to 500 μmol m^{-2} s^{-1}, light to 2000 μmol m^{-2} s^{-1}, and temperature to match ambient conditions which ranged between 23°C and 26°C. Once photosynthetic rates stabilized, we logged measurements every 5 s for 30 s (total = 6 per plant), and the infrared gas analyzer was matched between every plant. To control for variation of leaf area in the chamber, we measured the total leaf area contained within the chamber (using the LeafByte app, Getman-Pickering *et al*., 2020) and adjusted gas exchange measurements accordingly. We used R packages in RStudio (v.4.1.2; R Core Team, 2021) to average values of A_{sat} and E for each plant and then calculated leaf water-use efficiency (WUE_l) as A_{sat}/E (μmol CO_2 mmol H_2O^{-1}). Before subsequent analyses, we removed low-quality outlier data (e.g. nonreal negative values that could possibly be due to leaks and/or machine/user-errors; $n = 8$).

Statistical analyses

We examined our hypotheses with linear mixed-effect models and structural equation models (SEMs). In general, we analyzed GS influences on gas exchange properties separately for forbs and grasses, for C_3 and C_4 grasses without environmental variables (in linear mixed-effect models), or by excluding P/cell (in the SEM's) because we wanted to avoid both low statistical power issues associated with unbalanced designs and low sample sizes (e.g. N for: forbs = 377, grasses = 136, C_3 grasses = 52, C_4 grasses = 136, forb N/cell = 340, grass N/cell = 120, forb P/cell = 209, and grass P/cell = 59) and difficulties in interpreting complex significant three-way interactions. We believed that complex interactions were likely given that: the distribution of GS varies among lifeforms, environments, and C_3/C_4 grasses (see results, Bures *et al*., 2024); lifeforms and C_3/C_4 grasses have different stomata, root, and vein morphologies that have been correlated with differences in gas exchange rates (Ueno *et al*., 2006; Franks & Farquhar, 2007; Taylor *et al*., 2012; Harrison *et al*., 2020; Zhou *et al*., 2021, 2022; Chen *et al*., 2023); and lifeforms and C_3/C_4 grasses can respond differently to nutrient enrichments and changes in MAP and MAT (Rubio *et al*., 2010; Song *et al*., 2011; You *et al*., 2017; Havrilla *et al*., 2022).

Linear mixed-effect models Before fitting linear mixed-effect models, we examined whether closely related lineages were more likely to have similar GS, indicating a phylogenetic signal in GS variation, which could shape the relationships of GS to response variables. We pruned an existing phylogeny (Qian & Jin, 2016) with the APE (Paradis & Schliep, 2019) and PHYTOOLS (Revell, 2011) packages in RStudio (v.4.1.2; R Core Team, 2021) to obtain three phylogenies: one for all the plants ($n = 513$), one for the 377 forbs (62 unique taxa) and one for the 136 grasses (16 unique taxa) in our dataset. Then, for all phylogenies, we used the *phylosig* function from PHYTOOLS to test for phylogenetic signals in GS by calculating Pagel's λ (Pagel, 1999), which is a scaling function and ranging from zero if traits are independently distributed on a phylogeny to one if traits are distributed according to Brownian Motion. Pagel's λ was evaluated for significance by likelihood ratio tests.

To test our hypotheses, we accordingly used models that either accounted for a significant phylogenetic signal in GS (phylogenetic generalized linear mixed (PGLM) models) or that did not (restricted maximum likelihood (REML) models); PGLM models were done using the PHYR package (Li *et al*., 2020) in RStudio (v.4.1.2; R Core Team, 2021) and REML models were done using the JMP Pro v.16.0 statistical software (SAS Institute, Cary, NC, USA). Cellular nutrients and A_{sat} and E were square-root transformed to meet model assumptions of normality and homoscedasticity of variances. Furthermore, GS was right-skewed and was log-transformed and MAP and MAT were each standardized to have a mean of zero and a SD of one. In all analyses, model factors of lifeform (forbs, grasses), GS, MAP, MAT, photosynthetic pathway (C_3, C_4), and treatment (Cont., N, P, and NP) were treated as fixed effects while site and block nested within site were treated as random effects. We first examined whether GS, treatment, lifeform, and/or their interactions influenced cellular C, N, and P contents, stomatal sizes, and stomatal densities. Then separately for forbs and grasses, we examined whether GS, treatment, MAP, MAT, and/or two-way interactions between GS and the other factors (treatment, MAP, and MAT) influenced A_{sat}, E, and WUE_l. Within grasses only, we also examined whether GS, treatment, photosynthetic pathway, and/or two-way interactions between GS and treatment and photosynthetic pathway influenced A_{sat}, E, and WUE_l.

Structural equation models To better tease apart any direct vs indirect effects that GS may have on A_{sat} and E (mediated by resource−investment tradeoffs and/or physiological constraints), we developed separate SEMs for forbs and grasses. The two models included identical paths and were fit separately to forbs and grasses. The paths included were as follows: (1) GS predicted by MAP and MAT; (2) N/cell predicted by GS, N treatment, and P treatment; (3) stomatal density predicted by GS; (4) stomatal size predicted by GS; (5) A_{sat} predicted by stomatal density, stomatal size, GS, N/cell, MAT, MAP, N treatment, and P treatment; and (6) E predicted by stomatal density, stomatal size, GS, N/cell, MAT, MAP, N treatment, and P treatment (Fig. S1). All variables were transformed as described above and standardized before model fitting to aid in comparison of fitted coefficients. SEM paths were fit as mixed-effects models with species identity as a random intercept term using the lmer function in the LME4 package (Bates *et al.*, 2015) and whole SEM's were fit with the psem function in the PIECEWISESEM package (Lefcheck, 2016) in RSTUDIO (v.4.1.2; R Core Team, 2021). Paths were considered significant at an alpha level of 0.05.

Results

Cellular nutrient investments and stomatal attributes

Across forbs and grasses combined, GS was found to be statistically phylogenetically constrained (k = 0.27, LR = 8.34, $P = 0.0039$) with GS (in pg), on average, being larger in grasses (ranging from 1.41 to 23.67, mean = 8.36, median = 5.14) than in forbs (ranging from 0.52 to 28.07, mean = 4.64, median = 2.91, Tables S2, S3). Therefore, we used PGLM models to examine whether GS, lifeform, and/or treatment influenced cellular nutrient contents and/or stomata sizes and densities. Cellular nutrient contents tended to increase with GS but the increase also depended upon lifeform and treatment. For instance, grasses had on average less [C]/cell than forbs (Table 1); however, this

Table 1 Parameter estimates from phylogenetically corrected mixed linear (PGLM) models for the fixed effects of genome size (GS), lifeform (forbs, grasses), and treatment (control = Cont., nitrogen-added = N, nitrogen and phosphorus-added = NP, phosphorus-added = P) and the random effects of site and block (site) on cellular carbon (C) and nitrogen (N) (sample size = 377) and phosphorus (P) (sample size = 136) contents.

	[C]/cell[a]			[N]/cell[b]			[P]/cell[c]		
Parameter	Estimate	|Z| score	*P*-value	Estimate	|Z| score	*P*-value	Estimate	|Z| score	*P*-value
Intercept	10.2854	6.6137	< 0.0001	1.8746	4.2872	< 0.0001	0.4720	2.1803	0.0292
GS	0.9804	1.1259	0.2240	0.4327	2.5269	0.0115	0.2916	3.1035	0.0026
Lifeform	−13.5061	4.3235	< 0.0001	−1.7750	2.1133	0.0346	0.2157	0.5890	0.5558
N	−0.0316	0.0501	0.9600	0.1358	0.8760	0.3810	−0.0421	0.8637	0.3878
P	0.4847	0.8120	0.4168	0.1324	0.9027	0.3667	0.1398	3.0941	0.0020
NP	0.5295	0.9018	0.3672	0.2842	1.9696	0.0489	0.0180	0.4065	0.6844
GS 9 Lifeform	6.8430	4.7239	< 0.0001	0.5811	1.9560	0.0505	−0.3104	2.1037	0.0354
GS 9 N	0.1037	0.2641	0.7917	0.1925	1.9992	0.0456	0.0008	0.0254	0.9797
GS 9 P	−0.3085	0.8558	0.3921	−0.0218	0.2468	0.8051	0.0244	0.8605	0.3895
GS 9 NP	−0.1848	0.5022	0.6155	0.0617	0.6833	0.4944	0.0903	3.2487	0.0012
Lifeform 9 N	−0.8559	0.6630	0.5073	0.2889	0.9100	0.3628	−0.0490	0.5255	0.5993
Lifeform 9 P	−1.3638	0.9542	0.3400	0.1448	0.4116	0.6806	0.1303	1.2469	0.2124
Lifeform 9 NP	−2.4392	1.8844	0.0595	−0.4563	1.4354	0.1512	0.2488	2.5983	0.0094
GS 9 Lifeform 9 N	0.2615	0.4015	0.6880	−0.2228	1.3933	0.1635	0.0617	1.2062	0.2277
GS 9 Lifeform 9 P	0.4916	0.6922	0.4888	−0.0917	0.5248	0.5997	−0.0348	0.6464	0.5181
GS 9 Lifeform 9 NP	1.1101	1.7069	0.0878	0.2240	1.4028	0.1607	−0.1352	2.5019	0.0124

Before analysis, GS was log +1 transformed, and [C]/cell, [N]/cell and [P]/cell were square-root transformed. Bold values indicate a significant effect at a = 0.05 and the intercept terms represent the predicted value of the dependent variable when categorical factors are at their reference levels ('forbs' and 'control treatment') and the continuous factor (GS) is set to zero, averaged across all the groups defined by the random effects. In the footnotes a, b, c the variance (*V*) and SD of random factors are given for taxa, taxa_ (indicating that a phylogenetic covariance matrix was used), site, block (site), and residual.

[a](*V*, SD) for [C]/cell: taxa = (17.210, 4.149), taxa_ = (0.000, 0.004), site = (3.397, 1.843), block(site) = (0.000, 0.001), residual = (2.095, 1.447).

[b](*V*, SD) for [N]/cell: taxa = (0.521, 0.722), taxa_ = (0.014, 0.120), site = (0.067, 0.260), block(site) = (0.000, 0.000), residual = (0.127, 0.357).

[c](*V*, SD) for [P]/cell: taxa = (0.045, 0.211), taxa_ = (0.003, 0.005), site = (0.066, 0.257), block(site) = (0.000, 0.000), residual = (0.007, 0.085).

discrepancy was most pronounced for small GS grasses as [C]/cell within grasses was positively and significantly correlated with GS (Fig. 2; Table 1). Larger GS plants and forbs also generally had greater [N]/cell and [P]/cell than smaller GS plants and grasses, although the difference in [P]/cell between lifeforms only occurred for larger GS plants as grass [P]/cell was less impacted by changes in GS then forbs (Fig. 2; Table 1). Furthermore, plants in N-added plots tended to have greater concentrations of N per cell and plants in P-added plots tended to have greater concentrations of P per cell, although patterns slightly varied by GS and lifeform (Table 1; Fig. S2). Lastly, plant GS was significantly negatively correlated with stomata density (parameter estimate = −4.1675, $P = 0.0038$) but positively correlated with stomata size (parameter estimate = 7.2119, $P < 0.0001$), although lifeforms did not significantly differ in these stomatal attributes (Table S4).

Gas exchange attributes

Genome sizes varied among and within different grass and forb species (Table S2), and within forbs, plants belonging to Acanthaceae, Caryophyllaceae, and Asteraceae had the largest genomes, whereas plants belonging to Apocynaceae, Rubiaceae, and Rosaceae had the smallest genomes (Table S3). However, despite this variation and in contrast to the combined data set, GS was not statistically phylogenetically constrained within either functional group (forbs: k = 0.21, LR = 2.69, $P = 0.1010$; grasses: k = 0.42, LR = 2.12, $P = 0.1457$), and therefore, we did not need to account for phylogenetic signals of GS in statistical analyses of gas exchange attributes.

In forbs, except for treatment having a significant effect on E and $\mathrm{WUE_l}$, no other factors nor interactions among factors significantly affected forb gas exchange properties (Table 2). Specifically, forbs in the NP-added plots had significantly lower E and greater $\mathrm{WUE_l}$ values than forbs in the other plots and forbs in the P-added plots had significantly lower $\mathrm{WUE_l}$ values than forbs in the control plots (Table 2). By contrast, GS influenced grass gas exchange properties in three significant ways. First, GS influenced A_{sat} dependent upon MAT (Table 2) with smaller GS grasses generally having higher A_{sat} values than larger GS grasses, especially at the coolest sites (Fig. 3). Second, $\mathrm{WUE_l}$ of grasses was a function of MAT, MAP, and GS (Fig. 3; Table 2). Specifically, smaller GS grasses had higher $\mathrm{WUE_l}$ values across both warmer and colder sites (Fig. 3) and at wetter and dryer sites (Fig. 3), although at the driest sites all grasses, irrespective of their GS, had high $\mathrm{WUE_l}$ values (Fig. 3). Third, larger GS C_4-grasses had higher $\mathrm{WUE_l}$ values than smaller GS C_4-grasses, while GS did not correlate with $\mathrm{WUE_l}$ of C_3 grasses (Table S5; Fig. 4). Furthermore, in comparison with control plots, grasses in the NP-added plots tended to have lower E but higher $\mathrm{WUE_l}$ values vs those in the N-added plots that had lower $\mathrm{WUE_l}$ values (Tables 2, S5). Lastly, C_3 grasses had lower A_{sat} and $\mathrm{WUE_l}$ values than C_4 grasses and grasses at wetter sites exhibited marginally significantly higher transpiration rates (Tables 2, S5; Fig. 4).

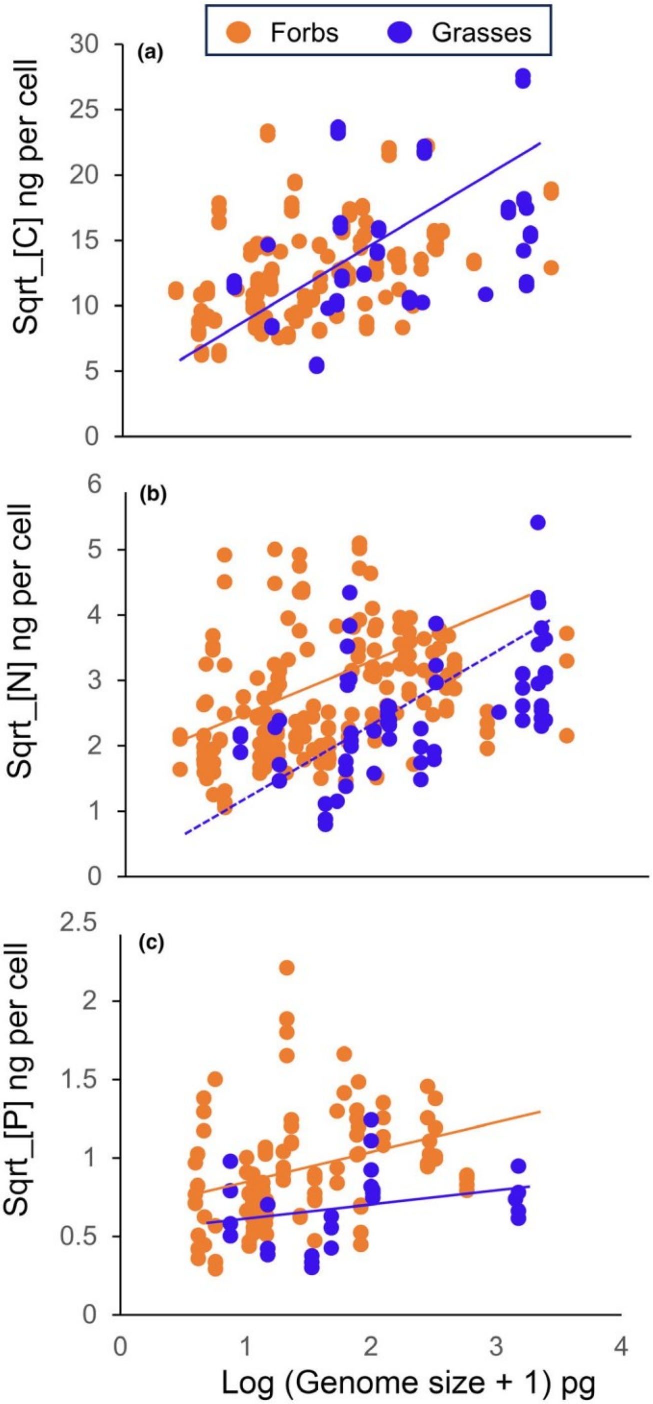

Fig. 2 Scatter plots of raw data displaying patterns from phylogenetically corrected mixed linear models between cellular carbon (C), nitrogen (N), and phosphorus (P) contents and genome sizes (GS) in picograms (pg) of forbs and grasses collected at seven nutrient network sites. Solid and dashed lines show relationships that are significant at $P < 0.01$ and $P = 0.05$, respectively. (a) [C]/cell increases with GS in grasses but is uncorrelated with GS for forbs (GS 9 Lifeform, $P < 0.0001$); (b) [N]/cell increases with GS generally (GS, $P = 0.0115$) but more steeply for grasses than for forbs (GS 9 Lifeform, $P = 0.0505$); (c) [P]/cell increases with GS generally (GS, $P = 0.0026$) but more steeply for forbs than grasses (GS 9 Lifeform, $P = 0.0354$). Full statistical details are in the text and Table 1.

Table 2 Parameter estimates from linear mixed (LM) models for the fixed effects of genome size (GS), treatment (control = Cont., nitrogen-added = N, nitrogen and phosphorus-added = NP, phosphorus-added = P), mean annual temperature (MAT), mean annual precipitation (MAP), two-way interactions with GS, and the random effects of site and block (site) on photosynthetic capacity (A_{sat}), transpiration (E), and leaf water-use efficiency (WUE_l) in forbs (sample size = 377) and grasses (sample size = 136).

	A_{sat}			E			WUE_l		
Parameter	Estimate	$\|t\|_{(den\_df)}$	Prob > t	Estimate	$\|t\|_{(den\_df)}$	Prob > t	Estimate	$\|t\|_{(den\_dfs)}$	Prob > t
A. Forbs[a]									
Intercept	3.5826	$10.90_{(9)}$	< 0.0001	2.5062	$10.26_{(8)}$	< 0.0001	2.5345	$10.52_{(11)}$	< 0.0001
GS	−0.1464	$1.19_{(353)}$	0.2342	−0.0600	$0.72_{(353)}$	0.4750	−0.0891	$0.91_{(352)}$	0.3617
N	−0.0435	$0.34_{(354)}$	0.7373	0.0066	$0.08_{(354)}$	0.9402	0.1616	$1.57_{(351)}$	0.1178
P	−0.0154	$0.12_{(352)}$	0.9040	0.0926	$1.07_{(353)}$	0.2869	−0.2425	$2.40_{(352)}$	0.0170
NP	0.0422	$0.34_{(350)}$	0.7333	−0.1981	$2.34_{(351)}$	0.0196	0.3674	$3.74_{(350)}$	0.0002
MAT	0.2659	$0.76_{(6)}$	0.4786	−0.0316	$0.12_{(5)}$	0.9094	0.2479	$0.98_{(6)}$	0.3622
MAP	0.1004	$0.31_{(4)}$	0.7710	0.5090	$2.05_{(4)}$	0.1061	−0.4901	$2.15_{(4)}$	0.0917
GS 9 N	0.1776	$0.84_{(349)}$	0.4017	0.0631	$0.44_{(349)}$	0.6623	−0.1716	$1.02_{(349)}$	0.3068
GS 9 P	0.0380	$0.19_{(350)}$	0.8504	0.0503	$0.37_{(350)}$	0.7149	−0.1152	$0.72_{(349)}$	0.4718
GS 9 NP	−0.0376	$1.59_{(351)}$	0.1137	−0.0583	$0.44_{(352)}$	0.6602	−0.2925	$1.90_{(350)}$	0.0584
GS 9 MAT	−0.3185	$1.12_{(358)}$	0.2615	−0.1988	$1.03_{(358)}$	0.3047	−0.0476	$0.21_{(355)}$	0.8334
GS 9 MAP	0.0738	$0.38_{(354)}$	0.7060	0.0511	$0.38_{(354)}$	0.7021	0.0299	$0.19_{(353)}$	0.8477
B. Grasses[b]									
Intercept	3.2647	$7.37_{(16)}$	< 0.0001	1.8178	$7.57_{(17)}$	< 0.0001	3.8361	$5.46_{(22)}$	< 0.0001
GS	0.1086	$0.57_{(90)}$	0.5725	0.0028	$0.03_{(104)}$	0.9772	0.1723	$0.57_{(102)}$	0.5684
N	−0.1667	$1.05_{(113)}$	0.2952	0.0497	$0.62_{(107)}$	0.5372	−0.8159	$3.22_{(112)}$	0.0017
P	−0.1600	$0.97_{(117)}$	0.3348	−0.0462	$0.55_{(111)}$	0.5825	0.0234	$0.09_{(116)}$	0.9296
NP	−0.0479	$0.31_{(117)}$	0.7599	−0.2062	$2.60_{(112)}$	0.0106	0.6263	$2.50_{(116)}$	0.0137
MAT	0.2515	$0.85_{(5)}$	0.4357	−0.2529	$1.37_{(5)}$	0.2261	1.3511	$2.68_{(7)}$	0.0317
MAP	−0.3393	$1.23_{(4)}$	0.2922	0.4589	$2.61_{(4)}$	0.0544	−1.6759	$3.56_{(5)}$	0.0150
GS 9 N	−0.2355	$1.16_{(112)}$	0.2472	−0.0820	$0.80_{(106)}$	0.4256	−0.2969	$0.92_{(111)}$	0.3614
GS 9 P	0.0599	$0.24_{(115)}$	0.8139	0.0547	$0.43_{(108)}$	0.6711	0.0935	$0.23_{(113)}$	0.8181
GS 9 NP	0.0340	$0.16_{(116)}$	0.8717	−0.0739	$0.69_{(113)}$	0.4914	0.2718	$0.81_{(116)}$	0.4216
GS 9 MAT	1.1778	$2.12_{(73)}$	0.0376	−0.2125	$0.76_{(99)}$	0.4501	2.0021	$2.29_{(91)}$	0.0241
GS 9 MAP	−0.5876	$1.53_{(107)}$	0.1285	0.2577	$1.33_{(118)}$	0.1874	−1.2653	$2.08_{(115)}$	0.0394

Before analysis, GS was log +1 transformed, MAT and MAP were standardized with mean = 0 and SD =1, and A_{max} and E were square-root transformed. Bold values indicate a significant effect at a = 0.05 and the intercept terms represents the predicted value of the dependent variable when the categorical factor is at the reference level ('control treatment') and the continuous factors (GS, MAT, and MAP) are set to zero, averaged across all the groups defined by the random effects. In the footnotes a, b are given the overall model fit and percent total variation accounted for by the random factors in the models.

[a] Overall model fit and % total variation accounted for by random factors for forb models for A_{sat}: R^2 = 0.24, % of total = 24.2%; E: R^2 = 0.43, % of total = 28.3%; WUE_l: R^2 = 0.44, % of total = 32.6%.

[b] Overall model fit and % total variation accounted for by random factors for grass models for A_{sat}: R^2 = 0.41, % of total = 23.9%; E: R^2 = 0.48, % of total = 35.9%; WUE_l: R^2 = 0.55, % of total = 27.2%.

Direct and indirect relationships

SEMs identified different combinations of direct and indirect relationships among the examined variables for forbs and grasses (Fig. 5). In forbs, increasing GS had a weak negative effect (−0.09) on A_{sat} mediated by cell N content, a product of opposing effects of GS on N/cell and of N/cell on A_{sat} (Fig. 5; Table S6). Addition of N to plots was also associated with increasing N/cell, reinforcing the effect of GS. However, even though GS was strongly related to stomatal size (Fig. 5; Table S6), the model resolved no other significant paths from stomatal traits to N/cell, A_{sat}, or E, indicating that stomatal variation in these forbs did not strongly predict the contributions of A_{sat} or E to forb WUE_l (Fig. 5; Table S6). Instead, A_{sat} was moderately, and E was strongly predicted by MAP, suggesting that variation in the physiological attributes of these forbs was predominantly related to site level mean precipitation (Fig. 5; Table S6). By contrast, in grasses although GS had strong positive effects on N/cell, GS effects on A_{sat} and E were mediated by stomatal traits rather than by N/cell. Specifically, increasing GS reduced A_{sat} (−0.18), which was a product of the opposing effects of GS on stomatal density and of stomatal density on A_{sat}. By contrast, increasing GS increased E (0.20) as a product of positive relationships between GS and stomatal size and stomatal size and E (Fig. 5; Table S6). Climate variables were unrelated to A_{sat} but reinforced the positive GS-E relationship because increasing MAP more strongly increased E than increasing MAT decreased E (Fig. 5; Table S6). Thus, larger GS grasses have lower WUE_l than smaller GS grasses, most notably in sites with high precipitation. No other model paths were significantly resolved in the forb and grass SEM's.

Discussion

The observation that angiosperm GS distribution is heavily skewed toward plants with smaller genomes (Dodsworth *et al.*, 2015) is puzzling. While traditional explanations of selection for functional traits (Mei *et al.*, 2018) and/or the fixation of

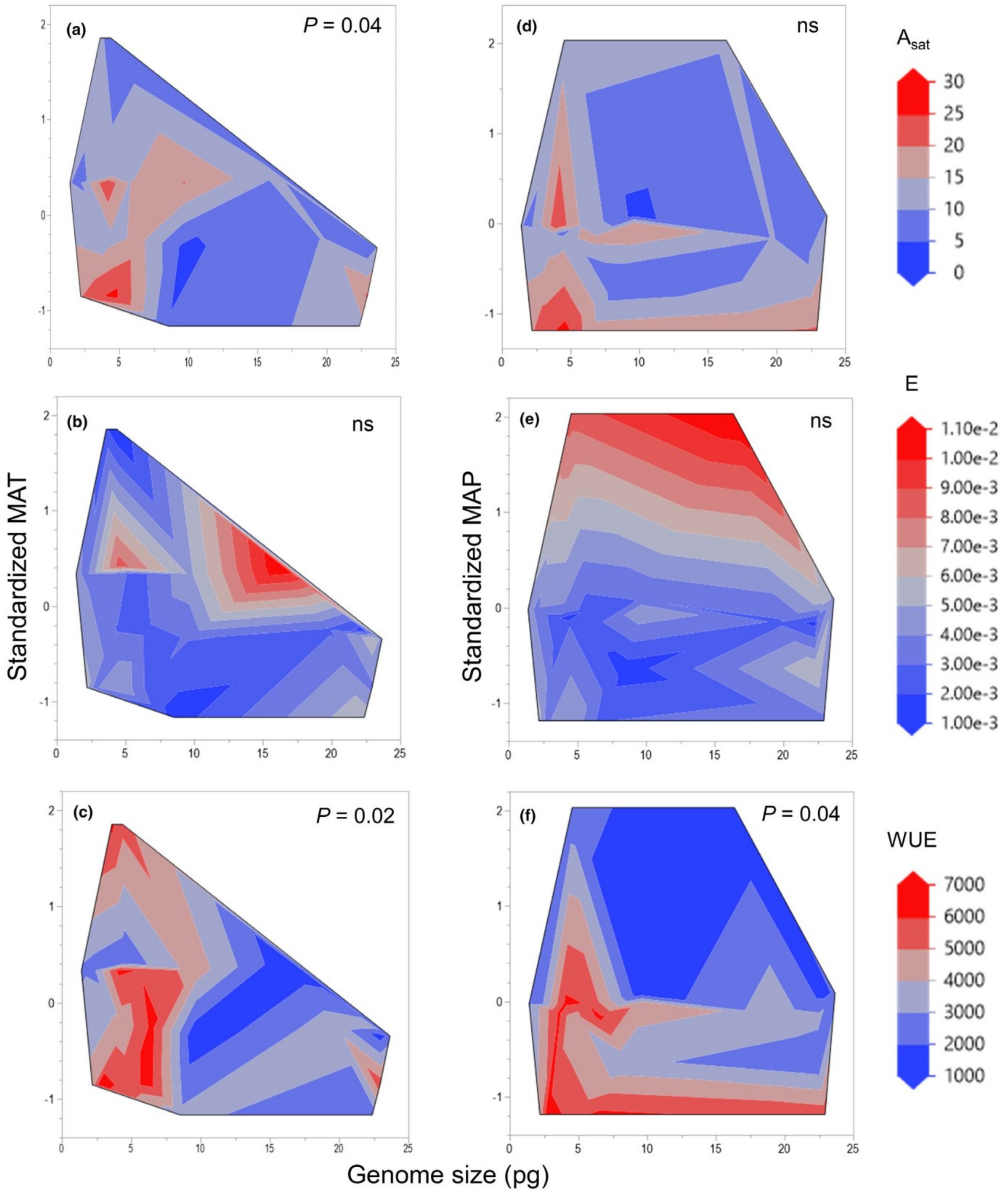

Fig. 3 Contour plots of raw data displaying patterns from mixed linear models of photosynthesis (A_{sat}, 1mol CO_2 m^{-2} s^{-1}), instantaneous transpiration rates (E, mmol H_2O m^{-2} s^{-1}) and leaf water-use efficiency (WUE_I, 1mol CO_2 mmol H_2O^{-1}) for grasses based upon their genome sizes (GS) in picograms (pg) and their sites standardized mean annual temperature (MAT, °C, a–c) or mean annual precipitation (MAP, mm yr^{-1}, d–f). Statistical significance of the interactions is given as the P-value or as ns for nonsignificant interactions and full statistical details are in the text and Table 2.

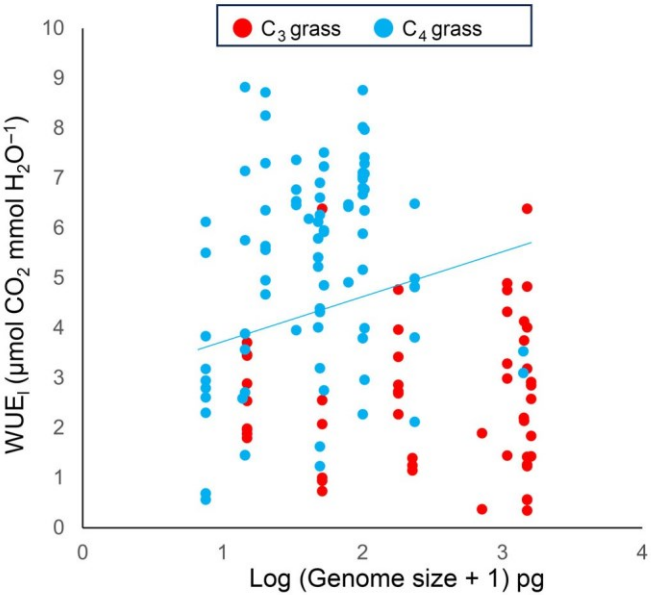

Fig. 4 Scatter plots of raw data displaying patterns from mixed linear models between leaf water-use efficiency (WUE$_I$, 1mol CO$_2$ mmol H$_2$O^{-1}) and genome size (GS) in picograms (pg) of C$_3$ and C$_4$ grasses collected at seven nutrient network sites. WUE$_I$ is generally higher in C$_4$ grasses (Photosynthetic pathway, $P < 0.0001$, indicated by the solid blue line) and increases with GS in C$_4$ grasses but not in C$_3$ grasses (GS 9 Photosynthetic pathway, $P = 0.0473$). Full statistical details are in the text and Supporting Information Table S5.

genomic rearrangement and deletions that promote stability (Wang *et al.*, 2021) likely explain most instances of genome downsizing, selection to reduce material costs of building genomes has also been proposed as a contributing influence (Lewis, 1985; Leitch & Bennett, 2004; Cavalier-Smith, 2005; Mei *et al.*, 2018; Faizullah *et al.*, 2021). Lending support to this hypothesis is research showing that plants with smaller genomes are selectively favored in nutrient-limiting environments (e.g. natural grassland studies: Smarda *et al.*, 2013; Guignard *et al.*, 2016; Peng *et al.*, 2022; Morton *et al.*, 2024; glasshouse studies: Bales & Hersch-Green, 2019; Walczyk & Hersch-Green, 2019; Anneberg & Segraves, 2020), that resource strategies can vary dependent upon GS (Bales & Hersch-Green, 2019; Wu *et al.*, 2019; Forrester *et al.*, 2020), and that selection on genomes and transcriptomes toward nutrient conserving substitutions can occur in nutrient-limited environments (Acquisti *et al.*, 2009a,b; Kelly, 2018; Majda *et al.*, 2021). However, it is not known: whether cellular material costs increase with GS across divergent plant species and thus whether nutrient constraints could impose stronger selective pressures on organisms with larger GS; nor whether associated GS-dependent resource–investment tradeoffs and/or nongenetic effects, such as physiological constraints associated with cell sizes and functioning (Bennett, 1971; Beaulieu *et al.*, 2008; Franks *et al.*, 2012; Simonin & Roddy, 2018; Roddy *et al.*, 2020; Théroux-Rancourt *et al.*, 2021) contribute to observed GS differences in growth responses to nutrients. Here, we examined plants from seven experimental grassland sites in which N and P soil levels were experimentally enriched or not to begin to assess these gaps. We found evidence that cellular nutrient contents increased with GS for phylogenetically divergent forb and grass species but GS effects on gas exchange properties were more nuanced, varying among species' evolutionary histories, lifeforms, nutrient fertilization treatments, and prevailing site climatic conditions. We discuss our results below referring to the potential ecological and evolutionary effects of plant GS *per se* on plant growth responses to varied environmental conditions.

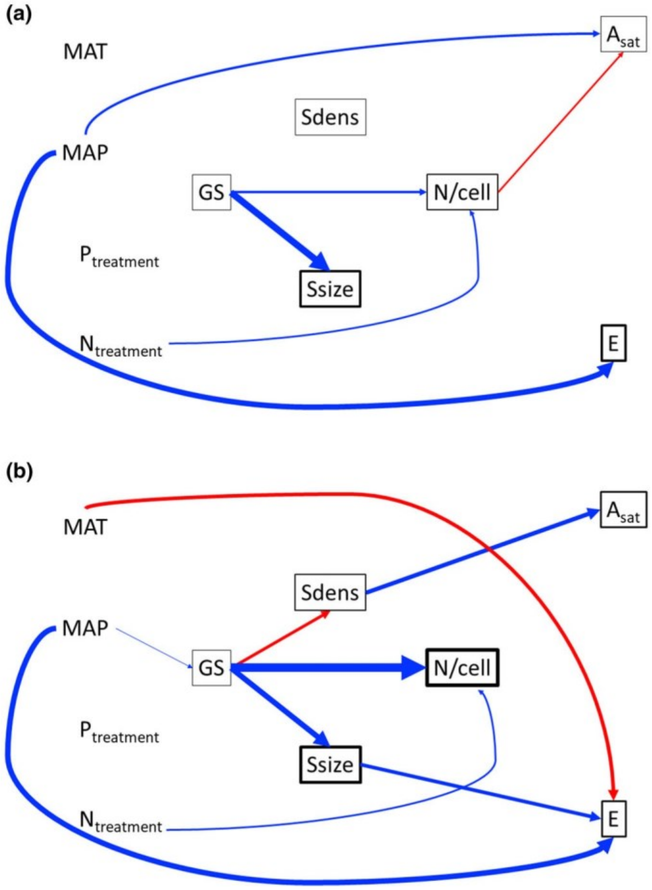

Fig. 5 Structural equation model (SEM) results for (a) forbs and (b) grasses. Arrows included are those that were significant ($P < 0.05$) following model fitting, where blue and red arrows indicate paths with positive and negative coefficients, respectively. Arrow width is proportional to the standardized coefficient of the path (see Supporting Information Table S5) and box width is proportional to the R^2 of the predicted variable. Key: A_{sat}, photosynthetic rate; E, transpiration rate; GS, genome size; MAP, mean annual precipitation of site; MAT, mean annual temperature of site; N/cell, nitrogen per cell; N$_{treatment}$, nitrogen addition treatment; P$_{treatment}$, phosphorus addition treatment; $S_{density}$, stomata density; S_{size}, stomata size.

Genome size effects on cell nutrient investments and evidence for material costs constraints

We found that cellular nutrient contents generally increased with increasing GS in both forbs and grasses. Such increases are thought to arise from the greater elemental costs of synthesizing longer DNA strands (Sterner & Elser, 2002; Elser *et al*., 2011) and phospholipid membranes associated with larger cells (Leitch & Bennett, 2004; Cavalier-Smith, 2005; Roddy *et al*., 2020). A previous study also found that cellular N and P contents increased with GS of the autopolyploid *Solidago gigantea* (from diploids to tetraploids to hexaploids, Walczyk & Hersch-Green, 2023); our findings are remarkable in that increases in cellular nutrient contents with GS were found for plants that are phylogenetically divergent and that grow in a wide range of climates and site conditions. Additionally, *post hoc* analysis of nutrients per mg of leaf tissue found that while N and P concentrations slightly increased with GS, that correlations between nutrient contents and GS were more muted and/or nonsignificant than those observed at the cellular levels (Table S7). Interestingly, previous studies have found both positive (Kang *et al*., 2015) and nonsignificant (Walczyk & Hersch-Green, 2023) associations between GS and foliar nutrient concentrations, and we believe that these more muted and nonsignificant GS-nutrient tissue level responses (such as observed here) most likely arise from tradeoffs between cell size and cell density per tissue area. Plants grown in plots with N-added and P-added also tended to have higher cellular N and P contents, respectively, suggesting that nutrient enrichments are incorporated into cells and that nutrient enrichments may contribute to the synthesis of additional nucleic acids, organelles, carbohydrates, fats, and/or proteins. By contrast, we found that [C] per mg leaf tissue decreased with GS (Table S7), and this may relate to differences in nutrient inputs as C was not added to plots.

Despite finding evidence that larger GS plants have increases in cellular nutrient contents, we did not find evidence to suggest that increased material costs influence resource allocation tradeoffs and gas exchange rates in either forbs or grasses. Thus, material cost constraints are unlikely to explain observed GS-dependent growth responses to nutrient fertilization. It should be noted, however, that material costs at the cellular level might not be indicative of material costs at the whole plant level. For example, plants vary in sizes, tissues vary in cell numbers and contents, and larger GS plants may have less cells per tissue (Beaulieu *et al*., 2008; Roddy *et al*., 2020) – all of which could offset increased nutrient costs per cell (Raven, 2013; Faizullah *et al*., 2021) and dampen resource allocation tradeoffs.

Genome size effects on stomata attributes and evidence for physiological constraints

In both forbs and grasses, we found that larger GS plants generally had fewer but larger stomata per leaf area than smaller GS plants, which could indirectly influence gas exchange rates (Franks & Farquhar, 2001; Franks & Beerling, 2009; Drake *et al*., 2013; Lawson & Blatt, 2014; Dittberner *et al*., 2018; Bertolino *et al*., 2019; Harrison *et al*., 2020; Zhang *et al*., 2022). However, support for the hypothesis that GS-dependent cell changes (e.g. to stomata size and functioning) influence gas exchange processes and could ultimately affect plant growth to nutrient enrichments varied between forb and grass plants.

In grasses, the relationship of GS to photosynthesis and WUE depended on site MAP and MAT. For instance, in alignment with our hypotheses, smaller GS grasses tended to have higher rates of photosynthesis, especially at cooler sites, and to be more water-use efficient, especially at cooler and dryer sites, than larger GS grasses. For several reasons we suspect that these patterns are attributed to how GS influences cell sizes, stomata functioning, and associated gas exchange rates rather than to increased material costs and stronger resource–investment tradeoffs in larger GS plants. First, GS differences in rates of photosynthesis were not more pronounced under nutrient-limiting conditions as would be expected if tradeoffs between cell and nucleic acid synthesis and photosynthesis largely explained observed patterns. In fact, we found no evidence that photosynthesis increased with nutrient enrichments. Other studies have reported null or species-specific photosynthesis responses to nutrient enrichments (Vaitkus *et al*., 1993; Lovelock *et al*., 2004; Liang *et al*., 2020; Shen *et al*., 2022). Second, despite larger GS forbs also having greater cellular nutrient investments, GS was not directly correlated with their photosynthesis responses. Instead, larger GS grasses had fewer stomata, and fewer stomata was directly correlated with lower rates of photosynthesis. Third, smaller GS grasses tended to be more water-use efficient than larger GS grasses in cooler and slightly dryer sites, and this pattern did not appear to be driven by resource–investment tradeoffs. Specifically, greater WUE of smaller GS grasses was a result of them having slightly higher rates of photosynthesis than larger GS grasses in cooler, dryer sites, in combination with lower transpiration rates in dryer sites; lower transpiration rates in dry climates have been reported for other species (Song *et al*., 2016). Lastly, if material costs largely explained patterns, then resource–investment tradeoffs should be more pronounced in C_4 grasses (especially in control plots) due to their greater nutrient investments into photosynthetic enzymes (Brown, 1978). However, independent of plot nutrient treatments, C_4 grasses had higher rates of photosynthesis and were more water-use efficient than C_3 grasses and within C_4 grasses WUE increased, not decreased, with GS. Other studies have also reported elevated photosynthesis and WUE rates of C_4 over C_3 grasses irrespective of nutrient availabilities and especially at dry sites (Monson, 1989; Sage, 2004; Taylor *et al*., 2010; Zhao *et al*., 2022). Such patterns may be because C_4 grasses continue to fix C despite closed stomata, have more numerous smaller stomata per leaf area, and have vein architectures that reduce transpiration rates – all of which have been correlated with differences in gas exchange rates and higher overall WUE (Ueno *et al*., 2006; Taylor *et al*., 2012; Harrison *et al*., 2020; Zhou *et al*., 2021, 2022; Chen *et al*., 2023).

Deviating from the overall patterns, at the driest site, larger GS grasses also displayed high WUE. As discussed above, this pattern most likely reflects the lower transpiration rates for all grasses at dry sites. The ability of larger GS grasses (and C_4 grasses in particular) to photosynthesize with higher WUE may allow them to grow more than smaller GS grasses in dry conditions or following nutrient enrichments, which could provide a mechanistic explanation as to why some larger GS plants (especially grasses) respond more positively to nutrient enrichments than smaller GS plants (Smarda *et al*., 2013; Guignard *et al*., 2016; Peng *et al*., 2022; Morton *et al*., 2024). For instance, plant growth is mostly accomplished by cell elongation rather than cell synthesis and larger GS plants with larger cell volumes might be able to expand their cells more than smaller GS plants with smaller cell volumes (Beaulieu *et al*., 2008). It should be noted that because we did not sample larger GS grasses at the warmest sites, we are not able to assess how GS affects photosynthesis, transpiration, and WUE rates of grasses at these sites.

By contrast, gas exchange properties in forbs were mostly influenced by the site's MAP and not by GS, suggesting limited support for physiological constraints affecting forb growth responses to nutrients. Specifically, forbs at wetter sites had much higher rates of transpiration than photosynthesis, which together resulted in these forbs having lower water-use efficiencies. Several studies have also noted that forbs, in comparison with grasses, are less impacted in terms of growth or photosynthesis by changes in nutrients, temperatures, and/or water availability (Song *et al*., 2011; Bai *et al*., 2015; You *et al*., 2017). The more muted responses of forbs vs grasses that we observed could be due to several factors. For instance, forbs have roots with more vessels and wider stele diameters (Zhou *et al*., 2021), which may enable them to store more nutrients and/or water than grasses (Dietz *et al*., 2020; Chen *et al*., 2023). Forbs and grasses also differ in stomata morphology and functioning; forbs have kidney-shaped guard cells, whereas grasses have dumbbell-shaped guard cells with additional subsidiary lateral cells, which are thought to make grass stomata more responsive (Franks & Farquhar, 2007; Chen *et al*., 2023). Thus, forbs may be better buffered whereas grasses may be more responsive and influenced by changing environmental conditions. Furthermore, although increasing GS was similarly correlated with larger stoma and presumably larger cells in both forbs and grasses, the generally larger stele diameters and the less responsive stomata of forbs may be less affected by changes in cell sizes, also contributing to their more muted responses. Lastly, in comparison with grasses, most of the forbs we sampled had smaller GS (their GS distribution was heavily skewed to the right), and thus, we may have had less power to detect GS-dependent responses within forbs.

Conclusion

The preponderance of small genomes in angiosperms has led to speculations that selection disproportionately favors small over large genomes (Lewis, 1985; Leitch & Bennett, 2004; Cavalier-Smith, 2005; Mei *et al*., 2018; Simonin & Roddy, 2018) and that increases in cellular nutrient investments might constrain GS evolution (Kang *et al*., 2015; Faizullah *et al*., 2021; Wang *et al*., 2021). Our results lend partial support to these hypotheses. We show that cellular nutrient investments increase with GS across widely divergent plant assemblages but that such increases are unlikely to be a major factor constraining plant growth and GS evolution. Instead, we suggest that changes in other attributes also associated with GS (such as cell sizes and stomata functioning) and/or with lifeforms (e.g. nutrient storage capacities and photosynthetic pathways) may more strongly influence GS-dependent growth responses to nutrients and abiotic site conditions. Because many different genomic processes contribute to changes in GS variation (e.g. retention and deletion of repetitive sequences, polyploidy), all of which can uniquely affect genomic and phenotypic traits, we suggest that additional studies should explore how GS in a range of lineages and climates affect primary and secondary metabolic attributes to better ascertain whether and how GS *per se* effects eco-evolutionary dynamics.

Acknowledgements

We thank Courtney Romes and Jeffrey Chieppa for data collection assistance, Jeffrey Chieppa, and Rob Tunison for assistance downloading and condensing Li-Cor data in R and site PIs for access to their experimental plots and hospitality (L. Biederman, E. Borer, L. Brudvig, K. Komatsu, R. McCulley, J. Nelson, E. Seabloom, and P. Wilfahrt). This work was funded by an NSF DEB CAREER grant awarded to E.I.H-G (Award # 1941309) and the Department of Biological Sciences at Michigan Technological University, Houghton, MI.

Competing interests

None declared.

Author contributions

EIH-G conceived and designed the study. EIH-G and HBH collected the data. EIH-G, HBH and NGS analyzed the data with input from PAF, EIH-G interpreted the data and wrote the first draft of the manuscript with revisions provided by all co-authors.

ORCID

Philip A. Fay https://orcid.org/0000-0002-8291-6316
Hailee B. Hass https://orcid.org/0000-0002-2749-2741
Erika I. Hersch-Green https://orcid.org/0000-0003-3887-0768
Nicholas G. Smith https://orcid.org/0000-0001-7048-4387

Data availability

The data that support the findings of this study are openly available on the Environmental Data Initiative (EDI) at: doi: 10.6073/pasta/38efe6bf0fdd5f0f7f6c22ff46cde50d and/or are available in the Supporting Information of this article. Code to reproduce results in R is freely available on GitHub: https://github.com/hpetosky/GenomeMetabolic.

References

Acquisti C, Elser JJ, Kumar S. 2009a. Ecological nitrogen limitation shapes the DNA composition of plant genomes. *Molecular Biology and Evolution* 26: 953–956.

Acquisti C, Kumar S, Elser JJ. 2009b. Signatures of nitrogen limitation in the elemental composition of the proteins involved in the metabolic apparatus. *Proceedings of the Biological Sciences* 276: 2605–2610.

Anneberg TJ, Segraves KA. 2020. Nutrient enrichment and neopolyploidy interact to increase lifetime fitness of *Arabidopsis thaliana*. *Plant and Soil* 456: 439–453.

Bai WM, Guo DL, Tian QY, Liu NN, Cheng WX, Li LH, Zhang WH. 2015. Differential responses of grasses and forbs led to marked reduction in below-ground productivity in temperate steppe following chronic N deposition. *Journal of Ecology* 103: 1570–1579.

Bales AL, Hersch-Green EI. 2019. Effects of soil nitrogen on diploid advantage in fireweed, *Chamerion angustifolium* (Onagraceae). *Ecology and Evolution* 9: 1095–1109.

Bates D, Mächler M, Bolker BM, Walker SC. 2015. Fitting linear mixed-effects models using lme4. *Journal of Statistical Software* 67: 1–48.

Beaulieu JM, Leitch IJ, Patel S, Pendharkar A, Knight CA. 2008. Genome size is a strong predictor of cell size and stomatal density in angiosperms. *New Phytologist* 179: 975–986.

Bennett MD. 1971. The duration of meiosis. *Proceedings of the Royal Society B: Biological Sciences* 178: 277–299.

Bertolino LT, Caine RS, Gray JE. 2019. Impact of stomatal density and morphology on water-use efficiency in a changing world. *Frontiers in Plant Science* 10: 225.

Borer ET, Harpole WS, Adler PB, Lind EM, Orrock JL, Seabloom EW, Smith MD. 2014. Finding generality in ecology: a model for globally distributed experiments. *Methods in Ecology and Evolution* 5: 65–73.

Brown R, Rickless P. 1949. A new method for the study of cell division and cell extension with some preliminary observations on the effect of temperature and of nutrients. *Proceedings of the Royal Society of London. Series B: Biological Sciences* 136: 110–125.

Brown RH. 1978. Difference in N use efficiency in C3 and C4 plants and its implications in adaptation and evolution. *Crop Science* 18: 93–98.

Bures P, Elliott TL, Vesely P, Smarda P, Forest F, Leitch IJ, Nic Lughadha E, Soto Gomez M, Pironon S, Brown MJM *et al*. 2024. The global distribution of angiosperm genome size is shaped by climate. *New Phytologist* 242: 744–759.

Cavalier-Smith T. 2005. Economy, speed and size matter: evolutionary forces driving nuclear genome miniaturization and expansion. *Annals of Botany* 95: 147–175.

Chen Z, Li H, Zhang WH, Wang B. 2023. The roles of stomatal morphologies in transpiration and nutrient transportation between grasses and forbs in a temperate steppe. *Annals of Botany* 132: 229–239.

Dietz S, Herz K, Gorzolka K, Jandt U, Bruelheide H, Scheel D. 2020. Root exudate composition of grass and forb species in natural grasslands. *Scientific Reports* 10: 10691.

Dittberner H, Korte A, Mettler-Altmann T, Weber APM, Monroe G, de Meaux J. 2018. Natural variation in stomata size contributes to the local adaptation of water-use efficiency in *Arabidopsis thaliana*. *Molecular Ecology* 27: 4052–4065.

Dodsworth S, Leitch AR, Leitch IJ. 2015. Genome size diversity in angiosperms and its influence on gene space. *Current Opinion in Genetics & Development* 35: 73–78.

Doležel J, Greilhuber J, Suda J. 2007. Estimation of nuclear DNA content in plants using flow cytometry. *Nature Protocols* 2: 2233–2244.

Drake PL, Froend RH, Franks PJ. 2013. Smaller, faster stomata: scaling of stomatal size, rate of response, and stomatal conductance. *Journal of Experimental Botany* 64: 495–505.

Elser JJ, Acquisti C, Kumar S. 2011. Stoichiogenomics: the evolutionary ecology of macromolecular elemental composition. *Trends in Ecology & Evolution* 26: 38–44.

Evans JR. 1989. Photosynthesis and nitrogen relationships in leaves of C3 plants. *Oecologia* 78: 9–19.

Faizullah L, Morton JA, Hersch-Green EI, Walczyk AM, Leitch AR, Leitch IJ. 2021. Exploring environmental selection on genome size in angiosperms. *Trends in Plant Science* 26: 1039–1049.

Fick SE, Hijmans RJ. 2017. WorldClim 2: new 1-km spatial resolution climate surfaces for global land areas. *International Journal of Climatology* 37: 4302–4315.

Forrester NJ, Rebolleda-Gomez M, Sachs JL, Ashman TL. 2020. Polyploid plants obtain greater fitness benefits from a nutrient acquisition mutualism. *New Phytologist* 227: 944–954.

Franks PJ, Beerling DJ. 2009. Maximum leaf conductance driven by CO2 effects on stomatal size and density over geologic time. *Proceedings of the National Academy of Sciences, USA* 106: 10343–10347.

Franks PJ, Farquhar GD. 2001. The effect of exogenous abscisic acid on stomatal development, stomatal mechanics, and leaf gas exchange in *Tradescantia virginiana*. *Plant Physiology* 125: 935–942.

Franks PJ, Farquhar GD. 2007. The mechanical diversity of stomata and its significance in gas-exchange control. *Plant Physiology* 143: 78–87.

Franks PJ, Leitch IJ, Ruszala EM, Hetherington AM, Beerling DJ. 2012. Physiological framework for adaptation of stomata to CO$_2$ from glacial to future concentrations. *Philosophical Transactions of the Royal Society of London. Series B: Biological Sciences* 367: 537–546.

Getman-Pickering ZL, Campbell A, Aflitto N, Grele A, Davis JK, Ugine TA. 2020. LeafByte: a mobile application that measures leaf area and herbivory quickly and accurately. *Methods in Ecology and Evolution* 11: 215–221.

Greilhuber J, Dolezel J, Lysak MA, Bennett MD. 2005. The origin, evolution and proposed stabilization of the terms 'genome size' and 'C-value' to describe nuclear DNA contents. *Annals of Botany* 95: 255–260.

Guignard MS, Nichols RA, Knell RJ, Macdonald A, Romila CA, Trimmer M, Leitch IJ, Leitch AR. 2016. Genome size and ploidy influence angiosperm species' biomass under nitrogen and phosphorus limitation. *New Phytologist* 210: 1195–1206.

Harrison EL, Arce Cubas L, Gray JE, Hepworth C. 2020. The influence of stomatal morphology and distribution on photosynthetic gas exchange. *The Plant Journal* 101: 768–779.

Havrilla CA, Bradford JB, Yackulic CB, Munson SM. 2022. Divergent climate impacts on C3 versus C4 grasses imply widespread 21st century shifts in grassland functional composition. *Diversity and Distributions* 29: 379–394.

Herben T, Suda J, Klimesova J, Mihulka S, Riha P, Simova I. 2012. Ecological effects of cell-level processes: genome size, functional traits and regional abundance of herbaceous plant species. *Annals of Botany* 110: 1357–1367.

Hessen DO, Jeyasingh PD, Neiman M, Weider LJ. 2010. Genome streamlining and the elemental costs of growth. *Trends in Ecology & Evolution* 25: 75–80.

Hohmann-Marriott MF, Blankenship RE. 2011. Evolution of photosynthesis. In: Merchant SS, Briggs WR, Ort D, eds. *Annual review of plant biology, vol. 62. Annual reviews.* Santa Clara, CA, USA: Palo Alto, 515–548.

Hull-Sanders HM, Johnson RH, Owen HA, Meyer GA. 2009. Influence of polyploidy on insect herbivores of native and invasive genotypes of *Solidago gigantea* (Asteraceae). *Plant Signaling & Behavior* 4: 893–895.

Jarvis PG, Mcnaughton KG. 1986. Stomatal control of transpiration – scaling up from leaf to region. *Advances in Ecological Research* 15: 1–49.

Jeyasingh PD, Weider LJ. 2007. Fundamental links between genes and elements: evolutionary implications of ecological stoichiometry. *Molecular Ecology* 16: 4649–4661.

Kang M, Wang J, Huang H. 2015. Nitrogen limitation as a driver of genome size evolution in a group of karst plants. *Scientific Reports* 5: 11636.

Kelly S. 2018. The amount of nitrogen used for photosynthesis modulates molecular evolution in plants. *Molecular Biology and Evolution* 35: 1616–1625.

Knight CA, Beaulieu JM. 2008. Genome size scaling through phenotype space. *Annals of Botany* 101: 759–766.

Lawson T, Blatt MR. 2014. Stomatal size, speed, and responsiveness impact on photosynthesis and water use efficiency. *Plant Physiology* 164: 1556–1570.

Lefcheck JS. 2016. PIECEWISESEM: piecewise structural equation modelling in R for ecology, evolution, and systematics. *Methods in Ecology and Evolution* 7: 573–579.

Leitch IJ, Bennett MD. 2004. Genome downsizing in polyploid plants. *Biological Journal of the Linnean Society* 82: 651–663.

Lewis WM. 1985. Nutrient scarcity as an evolutionary cause of haploidy. *American Naturalist* 125: 692–701.

Li DJ, Dinnage R, Nell LA, Helmus MR, Ives AR. 2020. phyr: an R package for phylogenetic species-distribution modelling in ecological communities. *Methods in Ecology and Evolution* 11: 1455–1463.

Liang X, Zhang T, Lu X, Ellsworth DS, BassiriRad H, You C, Wang D, He P, Deng Q, Liu H *et al*. 2020. Global response patterns of plant photosynthesis to nitrogen addition: a meta-analysis. *Global Change Biology* 26: 3585–3600.

Liu XL, Jiang FF, Wang ZW, Li XY, Li Z, Zhang XJ, Chen F, Mao JF, Zhou L, Gui JF. 2017. Wider geographic distribution and higher diversity of hexaploids than tetraploids in *Carassius* species complex reveal recurrent polyploidy effects on adaptive evolution. *Scientific Reports* 7: 1–10.

Lovelock CE, Feller IC, Mckee KL, Engelbrecht BMJ, Ball MC. 2004. The effect of nutrient enrichment on growth, photosynthesis and hydraulic conductance of dwarf mangroves in Panama. *Functional Ecology* 18: 25–33.

Majda S, Beisser D, Boenigk J. 2021. Nutrient-driven genome evolution revealed by comparative genomics of chrysomonad flagellates. *Communications Biology* 4: 328.

Marschner H. 2011. *Marschner's mineral nutrition of higher plants*. Cambridge, MA, USA: Academic Press.

Masson P, Dalix T, Bussière S. 2010. Determination of major and trace elements in plant samples by inductively coupled plasma-mass spectrometry. *Communications in Soil Science and Plant Analysis* 41: 231–243.

Mei W, Stetter MG, Gates DJ, Stitzer MC, Ross-Ibarra J. 2018. Adaptation in plant genomes: bigger is different. *American Journal of Botany* 105: 16–19.

Monson RK. 1989. The relative contributions of reduced photorespiration, and improved water-and nitrogen-use efficiencies, to the advantages of C3–C4 intermediate photosynthesis in Flaveria. *Oecologia* 80: 215–221.

Morton JA, Arnillas CA, Biedermann L, Borer ET, Brudvig LA, Buckley YM, Cadotte MW, Davies K, Donohue I, Ebeling A *et al*. 2024. Genome size influences plant growth and biodiversity responses to nutrient fertilization in diverse grassland communities. *PLoS Biology* 22: e3002927.

Mueller RL. 2015. Genome biology and the evolution of cell-size diversity. *Cold Spring Harbor Perspectives in Biology* 7: a019125.

Pagel M. 1999. The maximum likelihood approach to reconstructing ancestral character states of discrete characters on phylogenies. *Systematic Biology* 48: 612–622.

Paradis E, Schliep K. 2019. ape 5.0: an environment for modern phylogenetics and evolutionary analyses in R. *Bioinformatics* 35: 526–528.

Pellicer J, Hidalgo O, Dodsworth S, Leitch IJ. 2018. Genome size diversity and its impact on the evolution of land plants. *Genes* 9: 1–14.

Peng Y, Yang J, Leitch IJ, Guignard MS, Seabloom EW, Cao D, Zhao F, Li H, Han X, Jiang Y *et al*. 2022. Plant genome size modulates grassland community responses to multi-nutrient additions. *New Phytologist* 236: 2091–2102.

Qian H, Jin Y. 2016. An updated megaphylogeny of plants, a tool for generating plant phylogenies and an analysis of phylogenetic community structure. *Journal of Plant Ecology* 9: 233–239.

R Core Team. 2021. *R: A language and environment for statistical computing*. Vienna, Austria: R Foundation for Statistical Computing. [WWW document] URL https://www.R-project.org/.

Raven JA. 2013. RNA function and phosphorus use by photosynthetic organisms. *Frontiers in Plant Science* 4: 536.

Revell LJ. 2011. PHYTOOLS: an R package for phylogenetic comparative biology (and other things). *Methods in Ecology and Evolution* 3: 217–223.

Roddy AB, Théroux-Rancourt G, Abbo T, Benedetti JW, Brodersen CR, Castro M, Castro S, Gilbride AB, Jensen B, Jiang GF *et al*. 2020. The scaling of genome size and cell sizelimits maximum rates of photosynthesis with implications for ecological strategies. *International Journal of Plant Sciences* 181: 75–87.

Rubio G, Boem FHG, Lavado RS. 2010. Responses of C3 and C4 grasses to application of nitrogen and phosphorus fertilizer at two dates in the spring. *Grass and Forage Science* 65: 102–109.

Sage RF. 2004. The evolution of C4 photosynthesis. *New Phytologist* 161: 341–370.

Shen H, Dong S, Xiao J, Zhi Y. 2022. Effects of N and P enrichment on plant photosynthetic traits in alpine steppe of the Qinghai-Tibetan Plateau. *BMC Plant Biology* 22: 396.

Simonin KA, Roddy AB. 2018. Genome downsizing, physiological novelty, and the global dominance of flowering plants. *PLoS Biology* 16: e2003706.

Smarda P, Hejcman M, Brezinova A, Horova L, Steigerova H, Zedek F, Bures P, Hejcmanova P, Schellberg J. 2013. Effect of phosphorus availability on the selection of species with different ploidy levels and genome sizes in a long-term grassland fertilization experiment. *New Phytologist* 200: 911–921.

Song B, Niu SL, Wan SQ. 2016. Precipitation regulates plant gas exchange and its long-term response to climate change in a temperate grassland. *Journal of Plant Ecology* 9: 531–541.

Song L, Bao X, Liu X, Zhang Y, Christie P, Fangmeier A, Zhang F. 2011. Nitrogen enrichment enhances the dominance of grasses over forbs in a temperate steppe ecosystem. *Biogeosciences* 8: 2341–2350.

Sterner RW, Elser JJ. 2002. *Ecological stoichiometry: the biology of elements from molecules to the biosphere*. Princeton, NJ, USA: Princeton University Press.

Taylor SH, Franks PJ, Hulme SP, Spriggs E, Christin PA, Edwards EJ, Woodward FI, Osborne CP. 2012. Photosynthetic pathway and ecological adaptation explain stomatal trait diversity amongst grasses. *New Phytologist* 193: 387–396.

Taylor SH, Hulme SP, Rees M, Ripley BS, Woodward FI, Osborne CP. 2010. Ecophysiological traits in C3 and C4 grasses: a phylogenetically controlled screening experiment. *New Phytologist* 185: 780–791.

Théroux-Rancourt G, Roddy AB, Earles JM, Gilbert ME, Zwieniecki MA, Boyce CK, Tholen D, McElrone AJ, Simonin KA, Brodersen CR. 2021. Maximum CO_2 diffusion inside leaves is limited by the scaling of cell size and genome size. *Proceedings of the Royal Society B: Biological Sciences* 288: 20203145.

Ueno O, Kawano Y, Wakayama M, Takeda T. 2006. Leaf vascular systems in C3 and C4 grasses: a two-dimensional analysis. *Annals of Botany* 97: 611–621.

Vaitkus MR, Ciravolo TG, Mcleod KW, Mavity EM, Novak KL. 1993. Growth and photosynthesis of seedlings of 5 bottomland tree species following nutrient enrichment. *American Midland Naturalist* 129: 42–51.

Walczyk AM, Hersch-Green EI. 2019. Impacts of soil nitrogen and phosphorus levels on cytotype performance of the circumboreal herb *Chamerion angustifolium*: implications for polyploid establishment. *American Journal of Botany* 106: 906–921.

Walczyk AM, Hersch-Green EI. 2022. Do water and soil nutrient scarcities differentially impact the performance of diploid and tetraploid *Solidago gigantea* (Giant Goldenrod, Asteraceae)? *Plant Biology* 24: 1031–1042.

Walczyk AM, Hersch-Green EI. 2023. Genome-material costs and functional trade-offs in the autopolyploid *Solidago gigantea* (giant goldenrod) series. *American Journal of Botany* 110: e16218.

Wang X, Morton JA, Pellicer J, Leitch IJ, Leitch AR. 2021. Genome downsizing after polyploidy: mechanisms, rates and selection pressures. *The Plant Journal* 107: 1003–1015.

Wu SQ, Cheng JL, Xu XY, Zhang Y, Zhao YX, Li HX, Qiang S. 2019. Polyploidy in invasive *Solidago canadensis* increased plant nitrogen uptake, and abundance and activity of microbes and nematodes in soil. *Soil Biology & Biochemistry* 138: 107594.

Xu K, Guo L, Ye H. 2019. A naturally optimized mass transfer process: the stomatal transpiration of plant leaves. *Journal of Plant Physiology* 234–235: 138–144.

You C, Wu F, Gan Y, Yang W, Hu Z, Xu Z, Tan B, Liu L, Ni X. 2017. Grass and forbs respond differently to nitrogen addition: a meta-analysis of global grassland ecosystems. *Scientific Reports* 7: 1563.

Zhang M, Gao H, Chen S, Wang X, Mo W, Yang X, Wang X, Wang Z, Wang R. 2022. Linkages between stomatal density and minor leaf vein density across different altitudes and growth forms. *Frontiers in Plant Science* 13: 1064344.

Zhao YY, Lyu MA, Miao F, Chen G, Zhu XG. 2022. The evolution of stomatal traits along the trajectory toward C4 photosynthesis. *Plant Physiology* 190: 441–458.

Zhou M, Bai W, Li Q, Guo Y, Zhang WH. 2021. Root anatomical traits determined leaf-level physiology and responses to precipitation change of herbaceous species in a temperate steppe. *New Phytologist* 229: 1481–1491.

Zhou M, Guo Y, Sheng J, Yuan Y, Zhang WH, Bai W. 2022. Using anatomical traits to understand root functions across root orders of herbaceous species in a temperate steppe. *New Phytologist* 234: 422–434.

Supporting Information

Additional Supporting Information may be found online in the Supporting Information section at the end of the article.

Fig. S1 Hypothesized paths included in the structural equation models.

Fig. S2 Means and SE from raw data of [N]/cell and [P]/cell in pg for grasses and forbs in treatment plots.

Methods S1 Information on flow cytometry methods, including methods, buffers, and internal plant standards.

Table S1 Details on sites used in this study.

Table S2 Genome size information for the species that were included in this study.

Table S3 Information on families included in this study, including genome size (mean, minimum, maximum values) and the number of genera and individuals.

Table S4 Parameter estimates from PGLM models for the fixed effects of genome size and lifeform and the random effects of site and block(site) on stomata density and stomata size.

Table S5 Parameter estimates from LM models of grasses for the fixed effects of genome size, treatment, photosynthetic pathway, two-way interactions with genome size, and the random effects of site and block (site) on photosynthetic capacity, transpiration, and leaf water-use efficiency.

Table S6 Structural equation model results.

Table S7 Parameter estimates from PGLM models for the fixed effects of genome size, lifeform, treatment, and the random effects of site and block(site) on C, N, and P in mg per mg tissue.

Please note: Wiley is not responsible for the content or functionality of any Supporting Information supplied by the authors. Any queries (other than missing material) should be directed to the *New Phytologist* Central Office.